COMPDYN 2011
ECCOMAS Thematic Conference on
Computational Methods in Structural Dynamics and Earthquake Engineering
M. Papadrakakis, M. Fragiadakis, V. Plevris (eds.)
Corfu, Greece, 25-28 May 2011

STUDIES IN NUMERICAL STABILITY AND CRITICAL TIME STEP ESTIMATION BY WAVE DISPERSION ANALYSIS VERSUS EIGENVALUE COMPUTATION

Jiří Plešek[1], **Radek Kolman**[1], **and Dušan Gabriel**[1]

[1]Institute of Thermomechanics
Dolejškova 5, Praha 8, 182 00, Czech Republic
e-mail: plesek@it.cas.cz

Keywords: Explicit integration, Courant number, Critical time step, Wave propagation, Dispersion.

Abstract. *The critical Courant number limiting the length of time step in explicit integration schemes is inversely proportional to the maximum natural frequency of a finite element mesh. The well known recommendation* $\mathrm{Co} = 1$ *for linear finite elements is deemed to be best. In fact, for some configurations this choice may dangerously overestimate the critical time step. It was shown in an earlier paper that by increasing the number of elements in the finite element mesh one will paradoxically improve the mesh's stability towards its theoretical limit. The present paper refines some details, presenting small scale numerical tests. The first test involves a long truss/bar consisting of one row of elements whose critical Courant number changes as elements are added one after another. Since this increases the critical number one may pick up a time step such that it is supercritical to a certain mesh but becomes subcritical by merely adding one element. In a similar fashion, a square area is tested in the second example, using different arrangements of edge supports. It turns out that the numerical solutions to wave propagation may be strongly influenced by small variation of distant boundary conditions, which should normally be physically insignificant.*

1 INTRODUCTION

Detailed analysis of accuracy and stability of finite element wave propagation solutions was presented in review paper [1] and references cited therein for various finite elements including consistent and lumped mass matrices. The critical Courant number limiting the length of the time step in explicit integration schemes, namely the central difference method, follows from the famous formula

$$\mathrm{Co}_{\mathrm{crit}} = \frac{2}{\bar{\omega}} \tag{1}$$

where $\bar{\omega}$ is the dimensionless frequency

$$\bar{\omega} = \frac{\omega_{\max} H}{c_1} \tag{2}$$

with $\omega_{\max}$ being the maximum natural frequency of a finite element mesh, H the element size, and c_1 the speed of the fasted wave propagating in a continuum, typically the longitudinal wave. Nearly equally famous recommendation $\mathrm{Co} = 1$ (or slightly less to be on the safe side) for linear finite elements, also known to engineers as "rule of thumb" is deemed to be best. In fact, this observation comes from dispersion analysis but, as it has been shown in Ref. [1], for some configurations it may dangerously overestimate the critical time step. It was also shown that by increasing the number of elements, N, in the finite element mesh one will improve the mesh's stability towards $\mathrm{Co}_{\mathrm{crit}} = 1$ as $N \to \infty$, which is rather a paradoxical finding.

The present paper refines these details, presenting small scale numerical tests, which exemplify some peculiarities. The first test involves a long truss/bar consisting of one row of elements whose critical Courant number changes as elements are added one after another. Since this increases the critical number one may pick up a time step such that it is supercritical to a certain mesh but becomes subcritical by merely adding one element. In a similar fashion, a square area is tested in the second example, using different arrangements of edge supports. It turns out that the numerical solutions to wave propagation may be strongly influenced by small variation of distant boundary conditions, which should normally be physically insignificant. Finally, the third illustration shows the direct numerical results relevant to the above mentioned choices of sub and supercritical times steps.

2 PROBLEM DESCRIPTION

This section concerns with essentials of wave propagation in homogeneous solids, finite element technology and dispersion computation.

2.1 Propagation of waves in an elastic isotropic continuum

The ith equation of motion in linear elastodynamics reads

$$(\Lambda + G)u_{j,ji} + Gu_{i,jj} = \rho \ddot{u}_i \tag{3}$$

In this equation, Λ and G are Lamé's constants, ρ is the mass density and u_i is the ith component of the displacement vector. Furthermore, a comma placed before subscripts refers to spatial differentiation whereas the superimposed dots denote the time derivatives. The summation convention on repeated indices is assumed. The Lamé constants Λ, G may be related to engineering constants E, ν as

$$\Lambda = \frac{\nu E}{(1+\nu)(1-2\nu)}, \qquad G = \frac{E}{2(1+\nu)} \tag{4}$$

where E and ν are Young's modulus and Poisson's ratio.

In an unbounded isotropic continuum, two types of planar waves exist: the longitudinal wave and two transversal waves, featuring mutually orthogonal polarisation. The longitudinal wave propagates with the speed

$$c_1 = \sqrt{\frac{\Lambda + 2G}{\rho}} \tag{5}$$

The speed of the two transversal waves is

$$c_2 = \sqrt{\frac{G}{\rho}} \tag{6}$$

The standard continuum is said to be *non-dispersive*. This is, by d'Alembert's solution, because the wave profile (wavelength) does not affect the velocity of propagation.

As a special case, one may consider a plane harmonic solution to Eqn. (3) as

$$u_i = U_i(\mathbf{x}) \exp(\mathrm{i}k\ (\mathbf{p} \cdot \mathbf{x} \pm ct)) \tag{7}$$

or its equivalent form

$$u_i = U_i(\mathbf{x}) \exp(\mathrm{i}(\mathbf{k} \cdot \mathbf{x} \pm \omega t)) \tag{8}$$

where $\mathrm{i} = \sqrt{-1}$ is the imaginary unit; $\mathbf{x}$ is a position vector; t is time; k is the wave number; $\mathbf{p}$ is the unit normal to the wave front; $\mathbf{k}$ is the wave vector, $\mathbf{k} = k\mathbf{p}$; c is the phase velocity; ω is the angular velocity; and U_i is the ith component of the amplitude vector at the point defined by the position vector $\mathbf{x}$. For a given wavelength λ, the wave number k may be computed from

$$k = \frac{2\pi}{\lambda} \tag{9}$$

The phase velocity c is related to ω and k by

$$c = \frac{\omega}{k} \tag{10}$$

Finally, the group velocity c_g is defined as

$$c_g = \frac{\mathrm{d}\omega}{\mathrm{d}k} \tag{11}$$

In non-dispersive systems, c is a constant and since $\omega = ck$, we get $c_g = c$. Thus, in the absence of dispersion the group velocity equals the phase velocity. On the other hand, $c_g \neq c$ indicates dispersion.

2.2 Finite element method

Spatial discretization by the finite element of an elastodynamic problem introduces the ordinary differential system

$$\mathbf{M}\ddot{\mathbf{u}} + \mathbf{K}\mathbf{u} = \mathbf{R} \tag{12}$$

Here, $\mathbf{M}$ is the mass matrix, $\mathbf{K}$ the stiffness matrix, $\mathbf{R}$ is the time-dependent load vector, and $\mathbf{u}$ and $\ddot{\mathbf{u}}$ contain nodal displacements and accelerations. The element mass and stiffness matrices are given by

$$\mathbf{M}_e = \int_V \rho \mathbf{H}^T \mathbf{H}\, \mathrm{d}V \tag{13}$$

and

$$\mathbf{K}_e = \int_V \mathbf{B}^T \mathbf{C} \mathbf{B} \, \mathrm{d}V \tag{14}$$

where $\mathbf{C}$ is the elasticity matrix, $\mathbf{B}$ is the strain-displacement matrix, $\mathbf{H}$ stores the displacement interpolation functions and integration is carried over the element domain. Global matrices are assembled in the usual fashion. Under plane strain conditions, the elastic matrix $\mathbf{C}$ takes the form

$$\mathbf{C} = \frac{E}{1-\nu^2} \begin{bmatrix} 1 & \nu & 0 \\ \nu & 1 & 0 \\ 0 & 0 & \frac{1-\nu^2}{2(1+\nu)} \end{bmatrix} \tag{15}$$

The mass matrix defined by Eqn. (13) is called the consistent mass matrix.

Explicit integration methods, such as the central difference method discussed later, require the mass matrix inverted. Thus, it is advantageous to have it diagonal or *lumped.* In contrast to consistent matrices, which are uniquely defined by the variational formulation, lumping procedures are not strictly prescribed. The only common principle is the ability of FEM to assemble diagonal global matrix from the element mass matrices, thus, lumping may be performed on an element basis. Out of many methods rendering the mass matrix diagonal we shall refer to the simplest: the row sum method (RS) for bilinear elements and the Hinton-Rock-Zienkiewicz method (HRZ) for quadratic elements—see Ref [1].

In the subsequent analysis, a regular $H_x \times H_y$ mesh composed of plane rectangular elements is considered with H_x and H_y measuring the length of element edges aligned with coordinate axes. It proves useful to define reference matrices $\bar{\mathbf{M}}_e$, $\bar{\mathbf{K}}_e$ for a parent element having unit properties E and ρ, unit thickness b and unit length $H_x = 1$. Then performing integration over the reference domain $1 \times r$ one gets

$$\mathbf{M}_e = brH_x^2 \rho \bar{\mathbf{M}}_e \tag{16}$$

and

$$\mathbf{K}_e = bE\bar{\mathbf{K}}_e \tag{17}$$

Therefore, a class of problems is defined by two constants: the Poisson ratio ν and the aspect ratio $r = H_y/H_x$. Within this class, the reference stiffness matrix $\bar{\mathbf{K}}_e$ is a function of ν and r whereas the reference mass matrix $\bar{\mathbf{M}}_e$ is independent of both. Denote by $\bar{\omega}_e$ the maximum natural frequency of a *single* element described by these unit matrices. For example, one may compute $\bar{\omega}_e = 2.39$ for the bilinear RS elements or $\bar{\omega}_e = 7.61$ for the quadratic serendipity HRZ elements.

2.3 Dispersion computation

The smooth solutions, Eqn. (7) and (8), no longer apply to discretized system (12). In this case, the speed of propagation of an harmonic wave depends on its angular frequency. According to Ref. [1], such dependence may be manifested by the dispersion plot shown in Fig. 1. In general, dispersion behaviour is investigated by considering an harmonic wave train travelling through unbounded mesh, which may be accomplished by prescribing periodic boundary conditions. Thus, the normalized frequencies read off the plot actually represent the limit natural frequencies corresponding to a very large (theoretically infinite) finite element mesh.

As in the preceding section, denote by $\bar{\omega}_\lambda$ the supreme value of the normalized angular frequency in Fig 1, e.g. $\bar{\omega}_\lambda = 2.00$ for bilinear elements and $\bar{\omega}_\lambda = 7.37$ for quadratic elements. It is worth mentioning that $\bar{\omega}_\lambda < \bar{\omega}_e$ in every case. It should also be noted that the dispersion

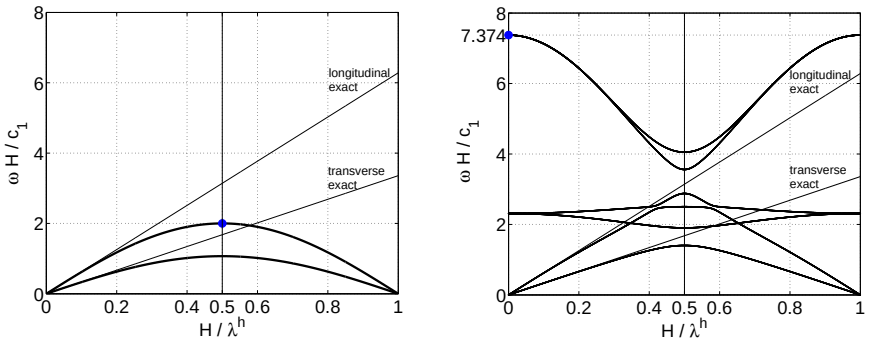

Figure 1: Dispersion curves for bilinear (left) and serendipity (right) elements.

diagrams discussed in this text are entirely due to spatial dispersion, neglecting effects of time integration—refer to paper [1] for complete treatise. This by no means oversimplifies actual problems since they are namely these theoretical values that enter stability criteria.

2.4 Explicit time integration and numerical stability

As a representative of explicit schemes, reviewed in Reference [2], the central difference method (CDM) will be discussed. Its discrete operator reads

$$\frac{1}{\Delta t^2}\mathbf{M}\mathbf{u}^{t+\Delta t} = \mathbf{R}^t - (\mathbf{K} - \frac{2}{\Delta t^2}\mathbf{M})\mathbf{u}^t - \frac{1}{\Delta t^2}\mathbf{M}\mathbf{u}^{t-\Delta t} \tag{18}$$

where $\mathbf{R}^t$ contains forces acting on the nodal points at time t. It is well known that CDM is only conditionally stable, Ref. [3], that is

$$\Delta t \leq \frac{2}{\omega_{\max}} \tag{19}$$

where $\omega_{\max}$ is the maximum eigenfrequency of the finite element mesh. The highest frequency can be computed by the standard FE software, aiming at the lowest eigenvalue with $\mathbf{K}$ and $\mathbf{M}$ swapped. This method was indeed employed in all the numerical computations presented here. Alternatively, the crititical time step may be estimated analytically as in Ref. [4].

At this point, it is convenient to introduce the Courant dimensionless number defined as

$$\mathrm{Co} = \frac{c_1 \Delta t}{H} \tag{20}$$

In elastodynamics, c_1 is the velocity of the longitudinal wave. Using the latter definition and that of $\bar{\omega}$ in Eqn. (2), the stability condition (19) can be rephrased as

$$\mathrm{Co} \leq \frac{2}{\bar{\omega}} \tag{21}$$

or, defining $\mathrm{Co}_{\mathrm{crit}}$, in the form of Eqn. (1). Inequality $\mathrm{Co} \leq 1$ then exactly manifests the Courant-Friedrichs-Levy stability condition for the linear truss element [2] but for other elements it may not be generally valid. On the other hand, we know, by Fried's theorem [5], which is a direct consequence of Sturm's polynomial separation property, that the maximum frequency is bounded by $\bar{\omega}_e$ obtained as the maximum eigevalue taken over all the elements in the FE mesh.

If the mesh is regular, composed only of rectangular elements of the same aspect ratio (the so-called structured mesh), one may devise another estimate of the critical time step, which lends some interesting insight into the problem of numerical stability in general. One asymptotic case arises for the infinite mesh, when $\omega_{\max}$ equals the supremum taken over all the dispersion curves for the particular element, i.e., $\bar{\omega}_\lambda$ is exploited. Tentatively, one may conjecture

$$\bar{\omega}_\lambda \leq \bar{\omega} \leq \bar{\omega}_e \tag{22}$$

This expression is indeed valid for an abitrary body with free boundary, $\Gamma_u = \emptyset$, but *does not hold* for a constrained mesh, for instance, if some displacement boundary conditions are prescribed. The meaning of the statement (22) will be clarified in full by examples shown in the next section.

Finally, it should be pointed out, that precisely because of the inequality (22), the true frequency of a real mesh will probably be higher than the estimate stemming from dispersion theory. Hence, the popular formula $c_1 \Delta t = H$ for the determination of time step length is not entirely safe.

3 NUMERICAL EXPERIMENTS

Unit dimensions were set in the numerical tests as follows: mass density $\rho = 1$, Poisson's ratio $\nu = 0.3$, and Young's modulus $E = 0.7428\ldots$ so that $c_1 = 1$ and $c_2 = 0.5345\ldots$. Furthemore, plane strain square bilinear elements with edge length $H = 1$ and unit thickness, $b = 1$, were employed. The reason for chosing linear rather than quadratic elements to illustrate stability properties is that the difference between $\bar{\omega}_\lambda = 2.00$ and $\bar{\omega}_e = 2.39$ is greater for these elements. Having N elements in the mesh, the total mass is $m = N\rho H^2 b = N$.

3.1 Plane strain bar

As the first example we consider a plane strain bar whose length is variable depending on the number of elements used. Fig 2 shows the eigenmode corresponding to the bar's maximum frequency for 40×1 discretization. The value of frequencies computed for various Ns are listed in Tab. 1.

Figure 2: Eigenvector corresponding to the highest frequency of a bar with free ends.

One important observation following the inspection of Tab. 1 is that starting from the 20×1 bar, the maximum frequency does not change within the first 8 digits, which suggests an existence of the limit. Alas, this limit, $\bar{\omega} = 2.16$, differs from the theoretical value $\bar{\omega}_\lambda = 2.00$. On the one hand, our sequence correctly starts at $\bar{\omega}_e = 2.39$ for 1×1 discretization, but on the other, the asymptotics $\mathrm{Co}_{\mathrm{crit}} = 1$ has never been reached. Why is it so? The answer lies in Fig 2. Since only the free ends vibrate, the maximum eigenvalue does not depend on the bar's length but solely on this boundary effect. The limit solution will not fit the periodical boundary conditions characteristic of the dispersion approach.

N	$\bar{\omega}$	$\mathrm{Co}_{\mathrm{crit}}$
1x1	2.3904568	0.8366602
2x1	2.1837346	0.9158622
3x1	2.1865457	0.9146848
4x1	2.1664669	0.9231620
5x1	2.1649080	0.9238268
6x1	2.1621023	0.9250256
7x1	2.1616266	0.9252292
8x1	2.1612303	0.9253988
9x1	2.1611334	0.9254403
10x1	2.1610747	0.9254654
20x1	2.1610454	0.9254780
40x1	2.1610454	0.9254780
80x1	2.1610454	0.9254780
100x1	2.1610454	0.9254780

Table 1: Critical Courant numbers for the bilinear finite element mesh of a free bar.

Another interesting observation follows from the graphical representation depicted in Fig. 3 on the log scale. Apart from the limit, there is a pronounced gap between the three and four element configurations. Selecting $\mathrm{Co} = 0.92$, the time step is stable for the 4×1 mesh but unstable for the smaller 3×1 mesh. This motivates the critical test defined in Fig. 4.

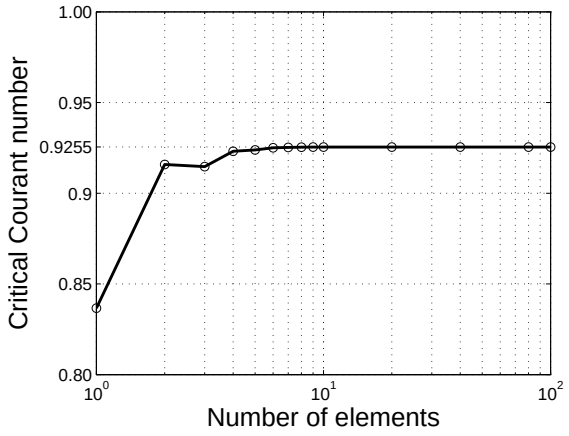

Figure 3: Distribution of the critical Courant number for the bar with free ends.

A three-element bar is loaded by the Heaviside step function $F(t) = 1$ for $t > 0$. Since $\mathrm{Co} = 0.92 > \mathrm{Co}_{\mathrm{crit}}$ one expects an incursion of instability after some time has elapsed but a stable solution if a four-element problem had been considered instead. In both the cases, parabolic displacement evolution

$$u(t) = \frac{F}{2m} t^2 = \frac{t^2}{2N} \tag{23}$$

applies to the motion of the whole body. The average acceleration, $1/N$, measured at the control point A for the 4×1 configuration equals 0.25. The existence of the stable solution is confirmed

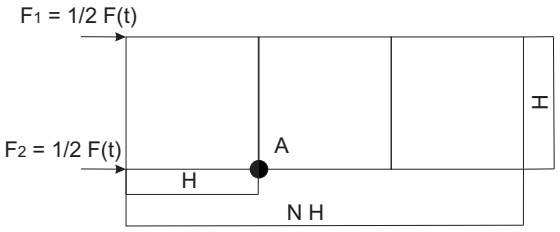

Figure 4: Transient problem with Heaviside load; unstable configuration.

by plots shown in Fig. 5. The oscillatory course of acceleration history is due to waves reflection about the mean value 0.25, which matches the rigid body motion. By contrast, the unstable 3×1

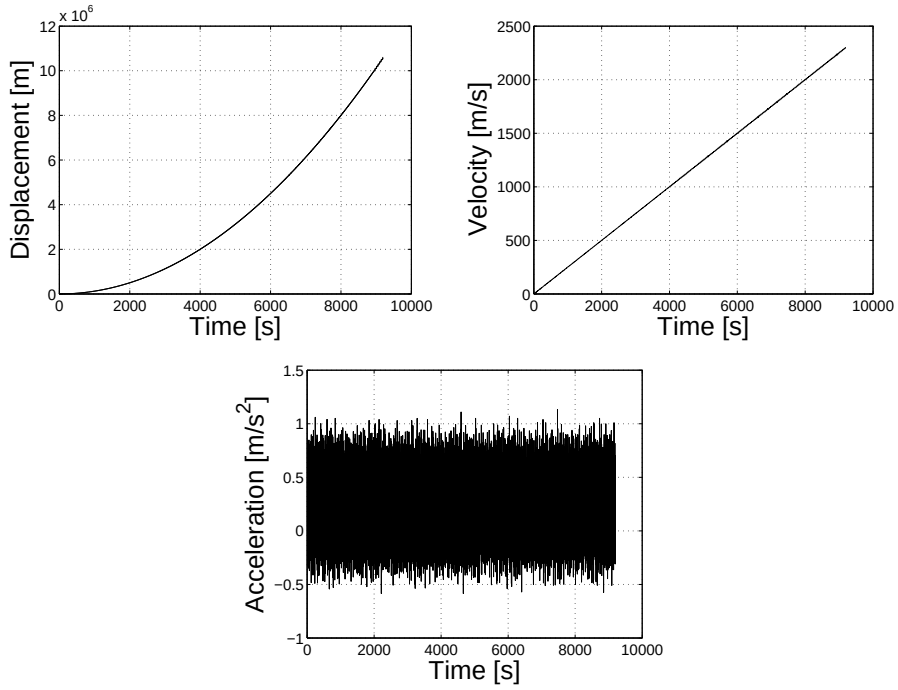

Figure 5: Displacement, velocity and acceleration in the stable 4×1 computation.

problem exhibits the solution's uncotrolled blow up at about $t = 3000$, see Fig. 6. The instability commences even much earlier after several wave reflections, which is nicely captured in Fig. 7.

Let us return to the original eigenvalue problem shown in Fig. 2. This time the boundary conditions are modified by clamping the right end. The corresponding eigenvector and the frequencies computed are shown in Fig. 8 and Tab. 2, respectively. The same limit $\bar{\omega} = 2.16$ is reached already by the 8×1 discretization, which is not surprising. Indeed, the vibration modes roughly correspond to those of the free bar twice the length of the free-fixed bar. A more interesting fact is that the maximum frequency now *increases*. This is because the results converge to the same limit as before but for each N-element bar the constrained configuration has lower maximum frequency than the free one. The critical Courant number distribution is shown in Fig. 9

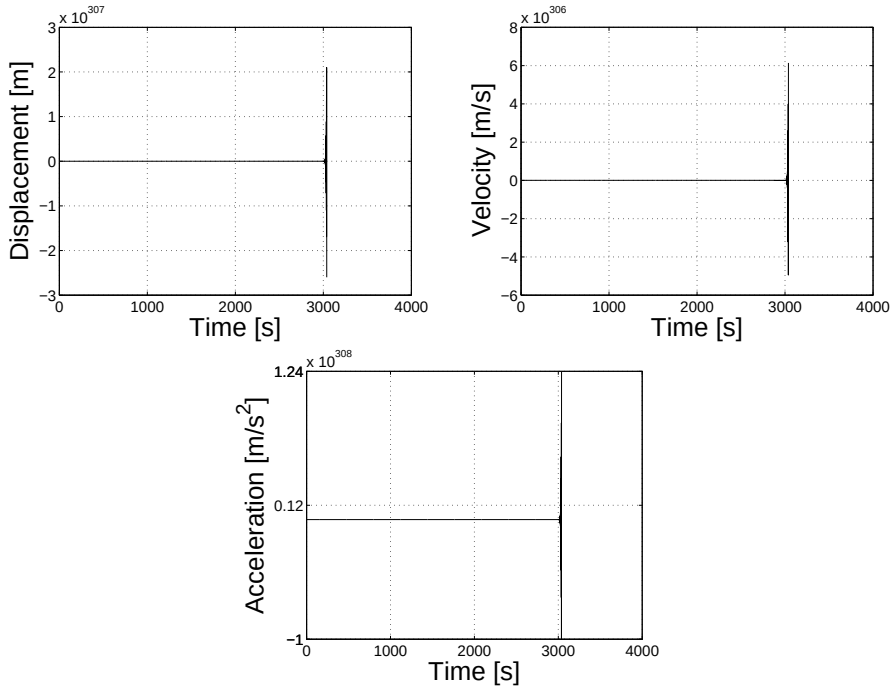

Figure 6: Displacement, velocity and acceleration in the unstable 3×1 computation.

N	$\bar{\omega}$	$\mathrm{Co}_{\mathrm{crit}}$
1x1	1.8403500	1.0867498
2x1	2.1530847	0.9288998
3x1	2.1587386	0.9264670
4x1	2.1608547	0.9255597
5x1	2.1609985	0.9254981
6x1	2.1610395	0.9254805
7x1	2.1610425	0.9254793
8x1	2.1610454	0.9254780
9x1	2.1610454	0.9254780
10x1	2.1610454	0.9254780
20x1	2.1610454	0.9254780
40x1	2.1610454	0.9254780
80x1	2.1610454	0.9254780
100x1	2.1610454	0.9254780

Table 2: Critical Courant numbers for the free-fixed bar.

We close our discussion concerning this example with the remark that the conjecture (22) does not hold for a constrained problem. For example, for the free-fixed bar $\bar{\omega}_\lambda > \bar{\omega}_{1\times1}$, because the maximu frequency has been reduced by the imposition of the boundary condition. Theoretically, one could even have had $\bar{\omega} = 0$ if all the nodes had been fixed. By contrast, $\bar{\omega}_e$ always forms the upper bound.

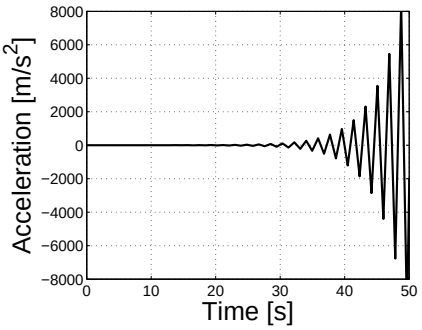

Figure 7: Detail of acceleration build up.

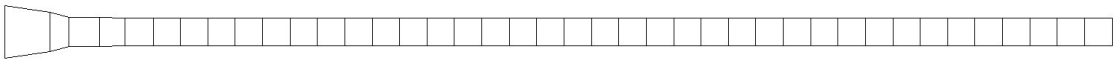

Figure 8: A free-fixed bar.

3.2 Plane strain square domain

Similar examples as in the preceding section may be analysed. Consider a plane strain square domain shown in Fig. 10 and the critical Courant number distributions for both (fixed and free) boundary configurations—Fig. 11.

In this case, convergence to the limit $\mathrm{Co}_{\mathrm{crit}} = 0.99$ is observed. Similarly as for the free bar this number is slightly less than the theoretical value $\mathrm{Co}_{\mathrm{crit}} = 1$. The reason can again been seen in Fig. 10, which suggests that it is the vibration of the corner elements that is responsible for the maximum frequency and is, in fact, independent of the mesh size.

A new phenomenon is detected with the constrained mesh. Comparing it with the free-fixed bar one notices that, here, zero displacements are prescribed along the whole boundary. This means that adding extra elements is merely equivalent to mesh refinement, which in turn implies the increase of the dimensionless maximum frequency. Since the mesh grading is regular and there are no boundary effects, monotonous convergence to the theoretical limit, $\mathrm{Co}_{\mathrm{crit}} = 1$, follows. It is interesting to note that also in this situation $\bar{\omega} < \bar{\omega}_\lambda$, which violates condition (22) as the present problem is fully constrained.

4 CONCLUSIONS

It might seem at first glance that, except illustrating certain mathematical principles, the present study bears little importance to real-world computation. On the one hand, todays engineering problems are extremely large (rendernig $N \to \infty$ effectively) and, on the other, one may safely use the upper bound by calculating the maximum eigenvalue of a single element.

It should be borne in mind that Fried's estimate, $\bar{\omega} \leq \bar{\omega}_e$, is only useful for a structured mesh when all the elements have the same spectrum. For an unstructured mesh, this information is hardly available and one must resort to other estimates. It is namely under such circumstances

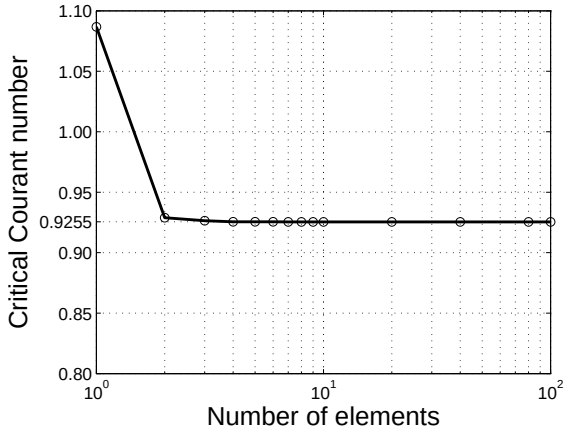

Figure 9: Distribution of the Critical Courant number for the free-fixed bar.

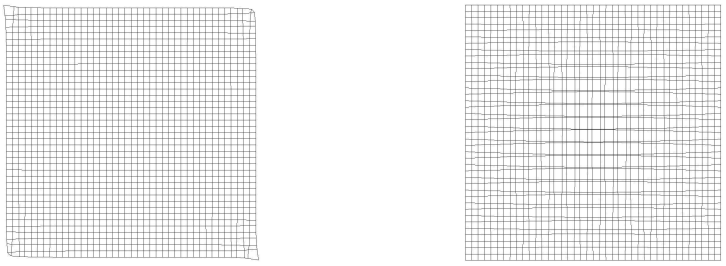

Figure 10: Maximum eigenmode of a free square domain (left) and the domain with fixed edges (right).

that the analysts use the $\bar{\omega}_\lambda$ limit derived from dispersion diagrams often unaware of its pitfalls. It must be emphasised that for the reasons exaplained in the paper the frequent recommendation $c_1 \Delta t = H$ is not entirely safe.

The examples involving free bodies clearly demonstrated the way the vibration of corner elements changed the stability limits. Hence, we conclude that even distant boundary conditions, which should normally be physically insignificant, may considerably influence numerical solution.

ACKNOWLEDGEMENTS

Support by GACR 101/09/1630, 101/07/1471 and GPP101/10/P376 under AV0Z20760514 is acknowledged.

REFERENCES

[1] J. Plešek, R. Kolman, D. Gabriel, Dispersion errors of finite element discretizations in elastodynamics. *Computational Technology Reviews Vol. 1, Saxe-Coburg Publications,* 251–279, 2010.

[2] M.A. Dokainish, K. Subbaraj, A survey of direct time-integration methods in computational structural dynamics - I: Explicit methods. *Computers & Structures*, **32**, 1371–1386, 1989.

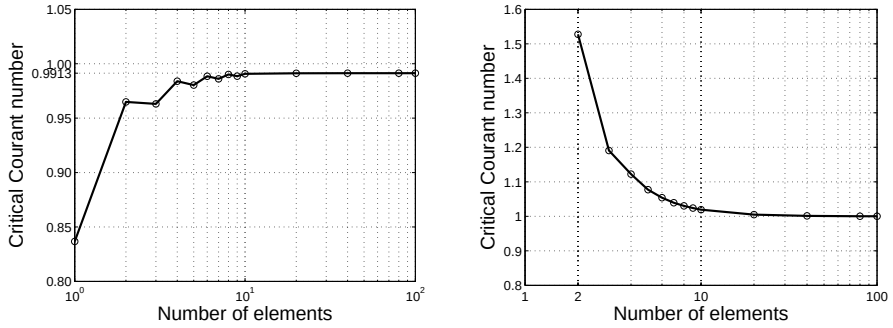

Figure 11: Critical Courant numbers for free (left) and fixed domain (right).

[3] K.C. Park, Practical aspect of numerical time integration. *Computers & Structures*, **7**, 343–353, 1977.

[4] D.P. Flanagan, T. Belytschko A uniform strain hexahedron and quadrilateral with orthogonal hourglass control. *Int. J. Num. Methods Engng.*, **17**, 679–706, 1981.

[5] I. Fried, Bounds on the extremal eigenvalues of the finite element stiffness and mass matrices and their spectral condition number. *Journal of Sound and Vibration*, **22**, 407–418, 1972.